

1 **Supplementary Data to "Modelling Interfacial** 2 **Dynamics Using Hydrodynamic Density Functional** 3 **Theory: Dynamic Contact Angles and the Role of** 4 **Local Viscosity"**

5 **B. Bursik¹†, R. Stierle¹, H. Oukili², M. Schneider², G. Bauer¹, and J. Gross¹**

6 ¹Institute of Thermodynamics and Thermal Process Engineering, University of Stuttgart,
 7 Pfaffenwaldring 9, 70569 Stuttgart, Germany

8 ²Institute for Modelling Hydraulic and Environmental Systems, University of Stuttgart,
 9 Pfaffenwaldring 61, 70569 Stuttgart, Germany

10 (Received xx; revised xx; accepted xx)

11 **1. Contact Angles Using the Bulk Viscosity Model**

12 Regarding velocity profiles and the velocity of the entire droplet, results from hydrodynamic
 13 DFT with the generalised entropy scaling model show much better agreement with NEMD
 14 results as compared to the bulk viscosity model (see the main text). In the following, we
 15 present results for dynamic contact angles using the bulk viscosity model.

16 The effect of the bulk viscosity model on density profiles is presented in figure 1. At
 17 the medium force ($f_x = 0.112$ pN, see figure 1c) the shape of the droplet shows slightly
 18 stronger deformations compared to NEMD (see figure 1d) and hydrodynamic DFT with
 19 entropy scaling (cf. the main text). This can be observed from the decreased height of the
 20 droplet and its increased width, i.e. the distance between the advancing and receding contact
 21 regions. For the lowest force ($f_x = 0.056$ pN, figure 1a and figure 1b) this effect can be
 22 observed to a lesser extent. At the largest external force studied here ($f_x = 0.224$ pN,
 23 figure 1e) the droplet, besides being more elongated, also shows a significantly non-spherical
 24 shape in strong contrast to results from NEMD (figure 1f). This manifests itself in an almost
 25 straight vapour-liquid interface in the top-centre of the droplet and an increased curvature at
 26 the contact regions, which also renders it difficult to determine the contact angle with the
 27 methodology described in the main text.

28 From these density profiles, contact angles for the bulk viscosity model are determined.
 29 They are contrasted to results from NEMD and hydrodynamic DFT with entropy scaling in
 30 figure 2. At the lowest force ($f_x = 0.056$ pN), the contact angles differ only slightly between
 31 hydrodynamic DFT with the two viscosity models. At the medium force ($f_x = 0.112$ pN)
 32 the receding contact angle is underestimated compared to NEMD. However, the advancing
 33 contact angle is overestimated. Consequently, the contact angle hysteresis $\Theta_a - \Theta_r = 51.6^\circ$
 34 is significantly larger for the simplified model than for both the NEMD results ($\Theta_a - \Theta_r =$
 35 35.5°) and hydrodynamic DFT with the entropy scaling model ($\Theta_a - \Theta_r = 34.5^\circ$). This is

† Email address for correspondence: bursik@itt.uni-stuttgart.de

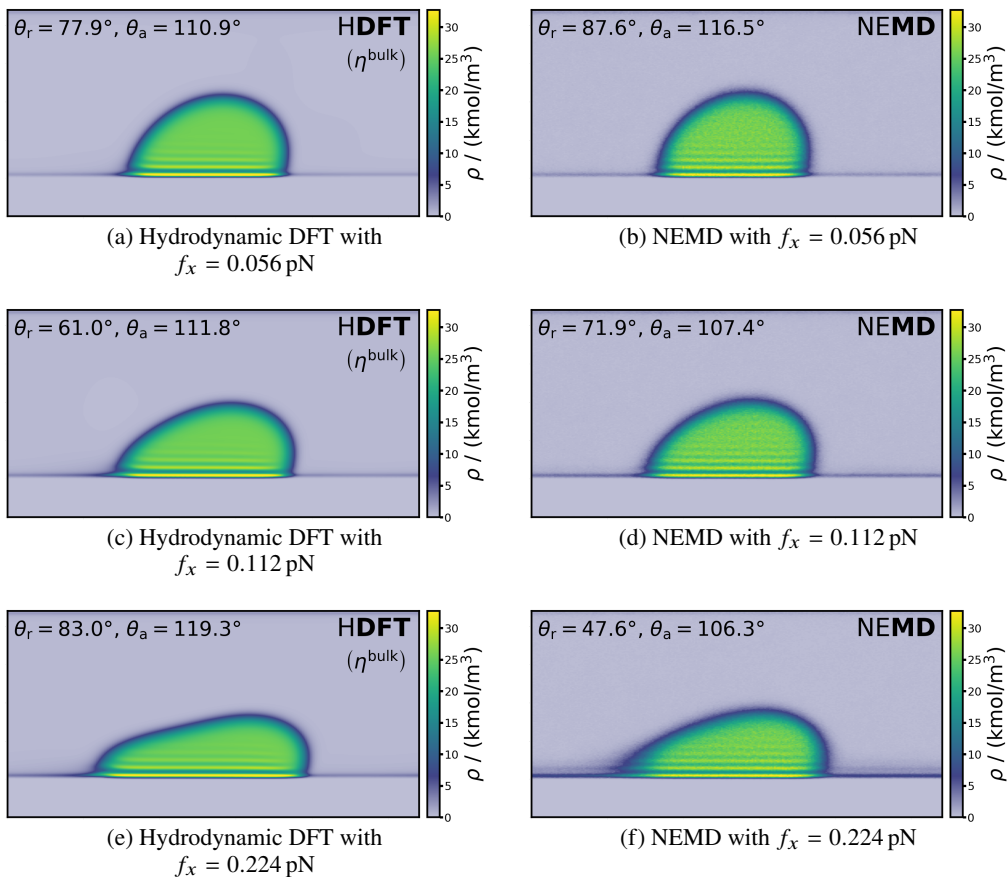


Figure 1: Density profiles of droplets moving along the solid-fluid interface with different external forces f_x from hydrodynamic DFT (HDFT) using the bulk viscosity model and from NEMD at $T = 120.02$ K with $\varepsilon_{\text{sf}}^* = 0.5$ averaged over 700 ps after a steady state is reached.

36 in agreement with the elongated shape of the droplet provided in figure 1c. At the largest
 37 force ($f_x = 0.224$ pN), the advancing contact angle again overestimates results from NEMD,
 38 whereas the receding contact angle deviates strongly from the other models. According to
 39 these results, density profiles and contact angles determined with the bulk viscosity model
 40 deviate from the other models. The deviations increase with increasing external force. As
 41 discussed in the main text, a plausible explanation for these results is that the simplified
 42 viscosity model does not provide an accurate description of the viscosity in the droplet.

43 2. Numerical Values for Dynamic Contact Angles

44 The numerical values for dynamic contact angles presented in this work are provided in
 45 table 1.

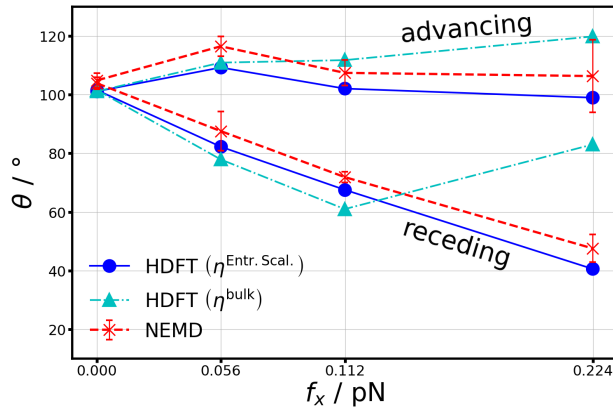


Figure 2: Summary of advancing and receding contact angles from hydrodynamic DFT with generalised entropy scaling viscosity model (blue points) and with the bulk viscosity model (light blue triangles) as well as from NEMD (red crosses) for different external forces at $T = 120.02$ K and with $\varepsilon_{sf}^* = 0.5$.

Section	Method	h/l_{cell}	ε_{sf}^*	$f_x = 0.0$ pN		$f_x = 0.056$ pN		$f_x = 0.112$ pN		$f_x = 0.224$ pN	
				Θ_{right}	Θ_{left}	Θ_a	Θ_r	Θ_a	Θ_r	Θ_a	Θ_r
4.5	HDFT + Entr. Scal.	0.5	0.5	101.1°	101.6°	109.3°	82.2°	102.1°	67.6°	99.0°	40.6°
	NEMD	0.5	0.5	104.9°	103.9°	116.5°	87.6°	107.4°	71.9°	106.3°	47.6°
Suppl. Data	HDFT + bulk	0.5	0.5	101.1°	101.6°	110.9°	77.9°	111.8°	61.0°	119.3°	83.0°
4.6	HDFT + Entr. Scal.	0.5	0.7	61.5°	63.6°	70.7°	42.0°	68.6°	24.3°	-	-
	NEMD	0.5	0.7	68.3°	65.8°	69.4°	43.5°	70.2°	22.5°	-	-
4.7	HDFT + Entr. Scal.	1.5	0.7	97.8°	98.1°	111.4°	80.0°	108.3°	64.5°	96.7°	38.1°
	NEMD	1.5	0.7	97.8°	94.3°	115.0°	77.2°	107.3°	61.4°	99.0°	28.2°

Table 1: Contact angles for different driving forces from hydrodynamic DFT (HDFT) using either the entropy scaling or the bulk viscosity model and from NEMD.

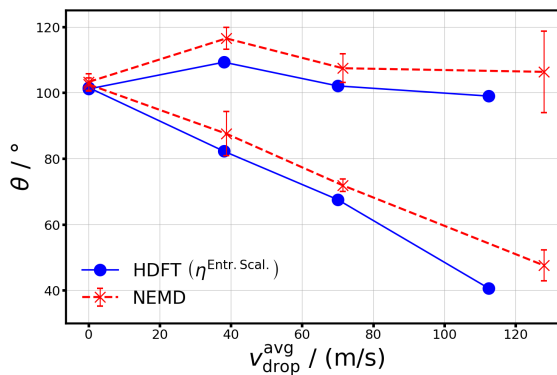


Figure 3: Contact angles as a function of the steady state velocity of the contact region from hydrodynamic DFT (HDFT) with entropy scaling viscosity model (circles) and from NEMD (crosses) at $T = 120.02$ K.

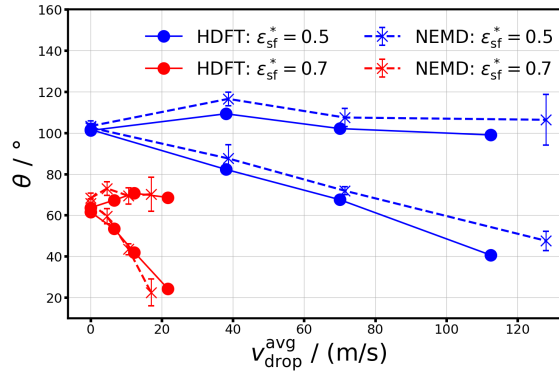


Figure 4: Contact angles as a function of the steady state velocity of the contact region for varying solid-fluid interaction parameter ϵ_{sf}^* from hydrodynamic DFT (HDFT) with entropy scaling viscosity model (circles) and from NEMD (crosses) at $T = 120.02$ K.

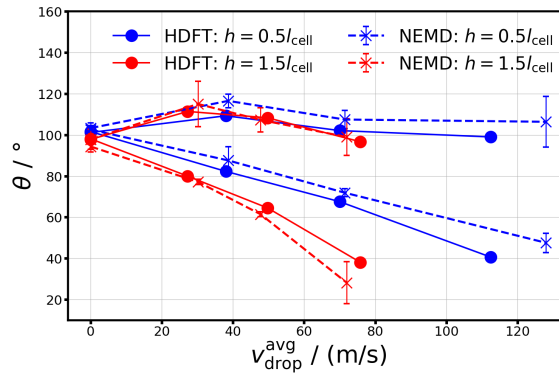


Figure 5: Contact angles as a function of the steady state velocity of the contact region for varying solid roughness h from hydrodynamic DFT (HDFT) with entropy scaling viscosity model (circles) and from NEMD (crosses) at $T = 120.02$ K.

46 3. Relation Between Contact Angles and Contact Region Velocity

47 Macroscopic studies are often concerned with the dependence of the (dynamic) contact
 48 angles on the velocity of the contact region (or contact line). At steady state the contact region
 49 moves with the same velocity as the centre of mass of the droplet. Thus, the dependence
 50 of contact angles on the velocity of the contact region can readily be visualised for the
 51 droplets studied in this work (see figures 3–5). Similar trends are observed as in the case
 52 where the contact angles are shown as a function of external force. This is expected, since
 53 the average velocity increases monotonically with the external force. In all cases (for varying
 54 solid-fluid interaction energy and varying solid roughness), the agreement between results
 55 from hydrodynamic DFT and NEMD is satisfactory.